Bioorganic & Medicinal Chemistry 20 (2012) 4310–4315

Contents lists available at SciVerse ScienceDirect

Bioorganic & Medicinal Chemistry

journal homepage: www.elsevier.com/locate/bmc

Quencher-free molecular beacon tethering 7-hydroxycoumarin detects targets through protonation/deprotonation

Hiromu Kashida, Kyohei Yamaguchi, Yuichi Hara, Hiroyuki Asanuma *

Graduate School of Engineering, Nagoya University, Furocho, Chikusa-ku, Nagoya 464-8603, Japan

ARTICLE INFO

Article history:
Received 23 April 2012
Revised 23 May 2012
Accepted 23 May 2012
Available online 1 June 2012

Keywords:
DNA
Fluorescence
7-Hydroxycoumarin
Molecular beacon
D-Threoninol

ABSTRACT

In this study, we synthesized a simple but efficient quencher-free molecular beacon tethering 7-hydroxycoumarin on D-threoninol based on its pK_a change. The pK_a of 7-hydroxycoumarin in a single strand was determined as 8.8, whereas that intercalated in the duplex was over 10. This large pK_a shift (more than 1.2) upon hybridization could be attributed to the anionic and hydrophobic microenvironment inside the DNA duplex. Because 7-hydroxycoumarin quenches its fluorescence upon protonation, the emission intensity of the duplex at pH 8.5 was 1/15 that of the single strand. We applied this quenching mechanism to the preparation of a quencher-free molecular beacon by introducing the dye into the middle of the stem part. In the absence of the target, the stem region formed a duplex and fluorescence was quenched. However, when the target was added, the molecular beacon opened and the dye was deprotonated. As a result, the emission intensity of the molecular beacon with the target was 10 times higher than that without the target. Accordingly, a quencher-free molecular beacon utilizing the pK_a change was successfully developed.

1. Introduction

A molecular beacon (MB) is a hairpin-shaped oligonucleotide probe that tethers a fluorophore and a quencher at its termini.[1] In the absence of the target, the stem part closes and the fluorophore and quencher interact with each other so that the emission is quenched. On the other hand, in the presence of the target, the MB opens and the fluorophore emits fluorescence. As a result, the target can be detected by the difference of the emission intensity with high sensitivity. To date, MBs have been widely used in SNP typing, real-time PCR, and mRNA imaging in living cells.[2] We have also proposed In-Stem Molecular Beacons, which tether a fluorophore and a quencher in the middle of the stem region.[3,4] However, these conventional MBs require at least two kinds of dyes, a fluorophore and a quencher, in order to quench emission in the absence of targets.

Recently, a novel class of molecular beacons that tethers no quencher but only fluorophore(s) has been reported.[5] Such quencher-free molecular beacons are advantageous over conventional ones due to their cost effectiveness and easy handling. In quencher-free MBs, the emission from the fluorophore(s) should change in the presence of the target. Several strategies have been reported for the emission change, such as quenching from nucleobases,[6–12] FRET,[13–18] excimer/exciplex formation,[19–21] and self-quenching of multiple fluorophores.[22] Here, we utilized a new strategy, quenching upon protonation, for the preparation of quencher-free MBs.

Previously, we incorporated several pH-sensitive dyes into DNA on D-threoninol and demonstrated that the dyes significantly changed their pK_as upon hybridization due to the more anionic environment in the DNA duplex.[23,24] For example, Brooker's Merocyanine, which is known to change both absorption and emission maxima upon protonation, shifted its pK_a from 9.5 to 10.1 upon duplex formation.[24] Although ratiometric detection of duplex formation was possible with this dye, its quantum yield was below 0.01, which severely limited the detection sensitivity. To overcome low emission, we utilized a new fluorophore, 7-hydroxycoumarin (**X** in Scheme 1), that has a quantum yield as high as 0.63 under basic conditions, and quenches its fluorescence upon protonation, to design more sensitive probe.[25,26] Seela et al. previously synthesized modified oligodeoxyribonucleotides (ODNs) tethering 7-hydroxycoumarin directly to nucleobases by using Click chemistry to locate it at the groove of the duplex.[27–30] In our case, D-threoninol is used as a linker to incorporate the dye into the middle of the ODN.[31] Previous NMR structural analyses revealed that dyes are intercalated between base pairs when they are introduced into DNA on D-threoninol.[23,32,33] Therefore, 7-hydroxycoumarin is expected to be located near the phosphate anions of the complementary strand between the base pairs. In addition, the hydrophobic environment should also promote the protonation of the dye, allowing an increase in pK_a of the dye upon hybridization. If the fluorescence is quenched simply by hybridization, 7-hydroxycoumarin is available for the preparation of quencher-free MBs. Here, we first investigated

* Corresponding author.
E-mail address: asanuma@mol.nagoya-u.ac.jp (H. Asanuma).

0968-0896/$ - see front matter © 2012 Elsevier Ltd. All rights reserved.
http://dx.doi.org/10.1016/j.bmc.2012.05.052

CXG: 5'-GGTATC**X**GCAATC-3'
cCXG: 3'-CCATAGCGTTAG-5'
MB1: 5'-GTCCTTGAGAAAGGGCTGCCATCAA**X**GGAC-3'
MB2: 5'-GTCCTTGAGAAAGGGCTGCCATCAAG**X**GAC-3'
MB3: 5'-GTCCTTGAGAAAGGGCTGCCATCA**X**AGGAC-3'
MB4: 5'-GTCCTTGAGAAAGGGCTGCCATC**X**AAG**X**GAC-3'
MBt: 5'-**X**GTCCTTGAGAAAGGGCTGCCATCAAGGAC-3'

Surv: 3'-CATCTCTACGCCACCAGGAACTCTTTCCCGACGGTC-5'

Scheme 1. Sequences of ODNs synthesized in this study. The chemical structure of 7-hydroxycoumarin (**X**) is also shown. Stem regions of MBs are underlined. The sequence of the target (**Surv**), which is complementary to MBs, is also underlined.

the spectroscopic behaviors of 7-hydroxycoumarin-modified ODNs in order to evaluate their structure, pK_a, and quenching efficiency. Then, we applied the quenching system to the preparation of quencher-free MBs.

2. Results and discussion

2.1. Synthesis of modified ODN with 7-hydroxycoumarin

The synthesis of phosphoramidite monomers tethering 7-hydroxycoumarin was conducted by using standard phosphoramidite chemistry (Scheme 2). First, 7-hydroxycoumarin was coupled to DMT-protected D-threoninol[4] (compound **1**). Then, the hydroxyl group of the dye was protected by an acetyl group and converted to a phosphoramidite monomer (compound **4**) for incorporation into ODN. After DNA synthesis, the acetyl group was successfully deprotected by treatment with ammonium hydroxide solution. The sequences of modified DNA are shown in Scheme 1.

Before evaluating the pK_a of 7-hydroxycoumarin, the stability of the duplex (**CXG**/**cCXG**) was evaluated at a different pH (Table 1). At pH 7.0, the melting temperature (T_m) of **CXG**/**cCXG** was 43.2 °C, which was 4.5 °C lower than that of the native duplex without the dye (47.7 °C). This destabilization is attributable to the small stacking area of 7-hydroxycoumarin. As listed in Table 1, the T_m was almost constant as a function of pH from 7 to 9.5, whereas it decreased to 27.7 °C at pH 10 due to the deprotonation of the imino protons of thymine and guanine. Accordingly, spectroscopic measurements were carried out below 20 °C, where the duplex is formed even at pH 10.

Then, we investigated the spectroscopic behaviors of **CXG** at pH 7.0 where 7-hydroxycoumarin is fully protonated. Single-stranded **CXG** showed a single peak at 330 nm attributable to the π–π^* transition of protonated 7-hydroxycoumarin, as shown in Figure 1. On the other hand, the addition of its complementary strand, **cCXG**, induced a small bathochromic shift (λ_{max} = 334 nm) and hypochromism of the band (Table 1, Figure 1). These spectral changes are caused by excitonic interactions between natural nucleobases and intercalated dyes.[34] CD spectra of **CXG**/**cCXG** showed symmetrical Cotton effects around 260 nm below 20 °C, demonstrating that the insertion of the **X** residue did not destroy the B-form duplex of natural nucleobases (Fig. 2). In addition, **CXG**/**cCXG** exhibited a small positive induced CD at 300–350 nm at 0 °C.

Table 1
Effects of pH on the melting temperature (T_m) of **CXG**/**cCXG** and absorption maxima of single-stranded **CXG** and **CXG**/**cCXG**

pH	T_m[a] (°C)	λ_{max}[b] (nm)	
		CXG	**CXG**/**cCXG**
7.0	43.2	330	334
8.0	43.1	331	334
8.5	42.7	333	335
9.0	40.9	369	335
9.5	39.2	371	335
10.0	27.7	371	341

[a] Solution conditions: [ODN] = 5.0 μM, [NaCl] = 100 mM.
[b] Absorption maxima at 0 °C.

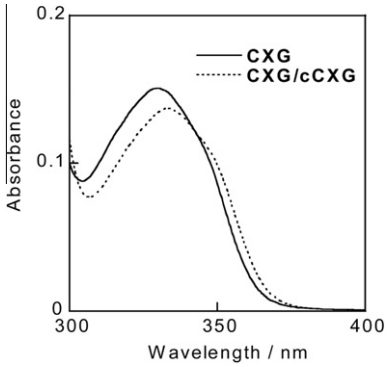

Figure 1. UV–Vis spectra of CXG and CXG/cCXG at pH 7.0. Solution conditions are as follows: [ODN] = 10.0 μM, [NaCl] = 100 mM, pH 7.0 (10 mM phosphate buffer), 0 °C.

Intercalated dyes are known to show much smaller ICD than groove-binder dyes.[35,36] Taken together, we concluded that 7-hydroxycoumarin is intercalated between base pairs.

2.2. Evaluation of pK_a change upon hybridization

Next, we investigated the effect of pH on the absorption spectra. Figure 3A shows the UV–Vis spectra of single-stranded **CXG** at various pH. At pH 7.01, a peak maximum was observed at 331 nm, which disappeared with pH increase, and concurrently a new peak

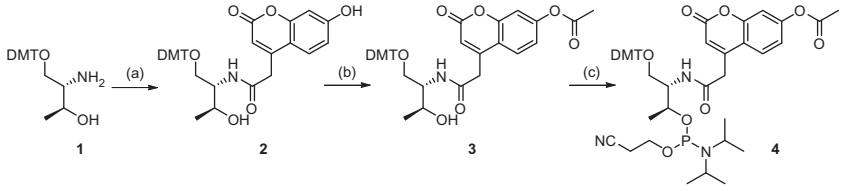

Scheme 2. Synthesis of phosphoramidite monomers tethering 7-hydroxycoumarin. Reagents and conditions: (a) 7-Hydroxycoumarinyl-4-acetic acid, PyBOP, Et_3N, CH_2Cl_2, rt, 3d, 94%; (b) acetic anhydride, *t*BuOK, THF, rt, overnight, 68%; (c) $(iPr)_2NP(Cl)(OCH_2CH_2CN)$, Et_3N, CH_3CN, 0 °C → rt, 1 h, quant.

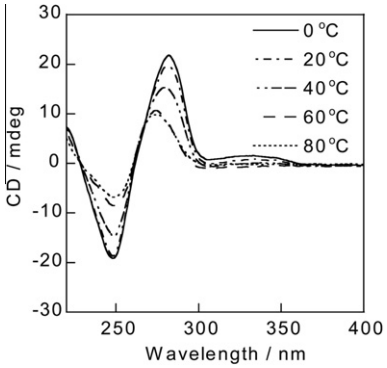

Figure 2. CD spectra of CXG/cCXG at various temperatures at pH 7.0. Solution conditions are as follows: [ODN] = 5.0 μM, [NaCl] = 100 mM, pH 7.0 (10 mM phosphate buffer).

assignable to the deprotonated dye appeared at 371 nm. From the titration curve monitored at 370 nm (Fig. 3B), the pK_a of the single-stranded **CXG** was determined as 8.8. Since the pK_a of 7-hydroxy-4-methylcoumarin is 7.8,[26] the introduction of 7-hydroxycoumarin into single-stranded DNA raised the pK_a by 1.0 units. This increase is probably caused by the anionic environment inside the DNA generated by phosphate anions.

Furthermore, pK_a significantly increased when the complementary strand, **cCXG**, was added to the solution. Figure 4A shows UV–Vis spectra of **CXG**/**cCXG** at various pH. In contrast to single-stranded **CXG**, the peak at 330 nm remained even at a pH higher than 10, demonstrating that the pK_a of **CXG**/**cCXG** is higher than that of single-stranded **CXG**. From the titration curve of **CXG**/**cCXG** shown in Figure 4b, pK_a was estimated to be over 10.0. Although the precise pK_a could not be determined due to the protonation of coumarin even at pH 10.0, its pK_a in the duplex was at least 1.2 higher than that in the single strand. The increase in pK_a upon duplex formation is much larger than that of merocyanine (9.5–10.1)[24] and Naphthyl Red (5.8–6.5).[23] Presumably, the smaller size of coumarin facilitated its accommodation between base pairs, resulting in the large increase in pK_a within the hydrophobic environment around the dye.

The change of pK_a by hybridization can be exploited for the detection of DNA hybridization. Figure 5 shows the absorption spectra of single-stranded **CXG** and **CXG**/**cCXG** at pH 8.5. At this pH, **CXG**/**cCXG** showed only a single peak at 335 nm assignable to protonated coumarin. On the contrary, single-stranded **CXG** gave a shoulder peak at about 370 nm, demonstrating that coumarin was partly deprotonated in the single-stranded state. Because the fluorescence emission of 7-hydroxycoumarin is quenched upon protonation, its emission should be lower upon hybridization. Actually, at pH 8.5, single-stranded **CXG** showed strong emission at 467 nm when excited at 365 nm where deprotonated coumarin has its λ_{max} (see solid line in Figure 6). On the other hand, hybridization with **cCXG** significantly lowered its emission (see dotted line in Fig. 6). As a result, the emission intensity of single-stranded

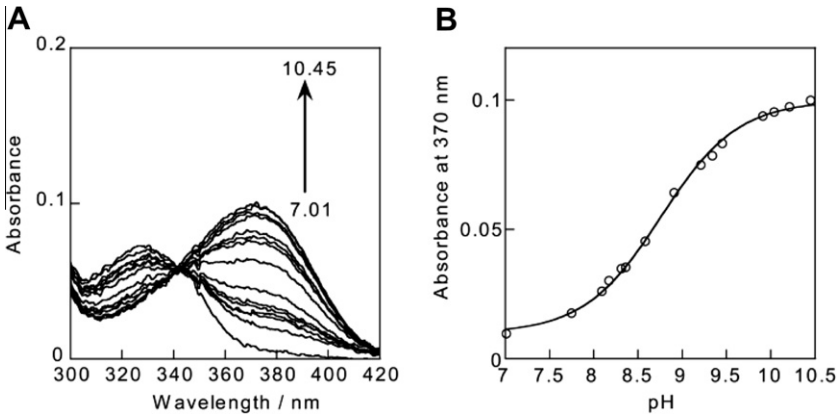

Figure 3. (A) UV–Vis spectra of **CXG** at various pH (from 7.01 to 10.45) and (B) plots of the absorbance of **CXG** at 370 nm as a function of pH at 20 °C. Solution conditions were as follows: [ODN] = 5.0 μM, [NaCl] = 100 mM, [NaH_2PO_4/Na_2HPO_4] = 10 mM.

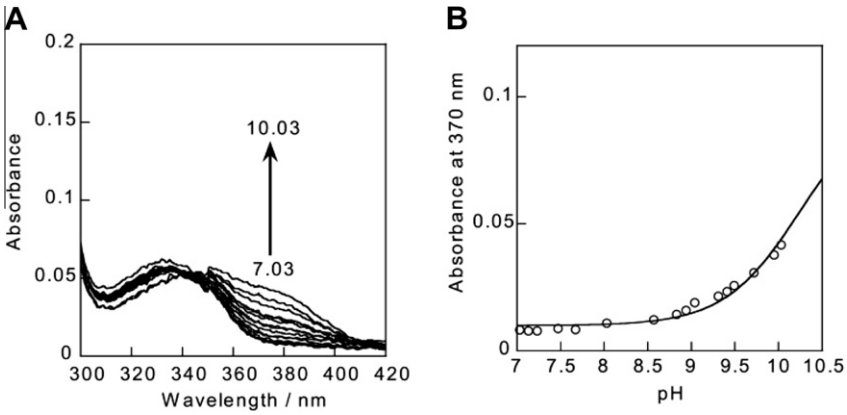

Figure 4. (A) UV–Vis spectra of **CXG**/**cCXG** at various pH (from 7.03 to 10.03) and (B) plots of the absorbance of **CXG**/**cCXG** at 370 nm as a function of pH at 20 °C. Solution conditions are as follows: [ODN] = 5.0 μM, [NaCl] = 100 mM, [NaH_2PO_4/Na_2HPO_4] = 10 mM.

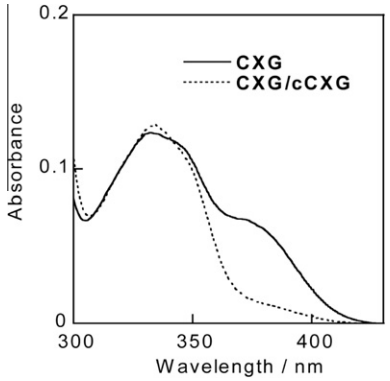

Figure 5. UV–Vis spectra of **CXG** (solid line) and **CXG/cCXG** (dotted line) at pH 8.5. Solution conditions were as follows: [ODN] = 10.0 μM, [NaCl] = 100 mM, pH 8.5 (10 mM Tris buffer), 0 °C.

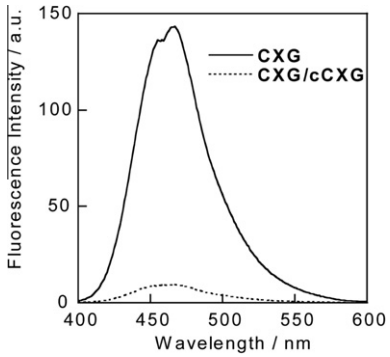

Figure 6. Fluorescence emission spectra (365 nm excitation) of **CXG** (solid line) and **CXG/cCXG** (dotted line) at pH 8.5. Solution conditions were as follows: [ODN] = 5.0 μM, [NaCl] = 100 mM, pH 8.5 (10 mM Tris buffer), 0 °C. The excitation wavelength was 365 nm.

CXG was 15.3 times higher than that of **CXG**/**cCXG**. In addition, strong emission of coumarin was observed in the single-stranded **CXG** at pH higher than 7.0 (see Fig. S1 in Supplementary data). Accordingly, duplex formation was successfully monitored with a negative response to the target by using coumarin-modified DNA. We also examined the sequence dependence on the emission spectra (see Fig. S2 in Supplementary data), and found that duplex dissociation could be monitored irrespective of the neighboring bases, although the ratio of the intensities between the single strand and duplex slightly depended on the sequence.

According to Seela et al., if the dye is attached to the 5 position of pyrimidines or the 7 position of purines, it results in localization at the groove of the duplex.[27–30] In this case, the pK_a of the dye should not change because the dye is located in a relatively hydrophilic environment, even in the duplex. In the studies of Seela et al., the difference in emission intensities between single strands and duplexes was not very large, although they did not determine each pK_a directly. In our design, the dye was introduced on D-threoninol to facilitate its intercalation between the base pairs. As mentioned above, UV–Vis and CD spectra showed that 7-hydroxycoumarin was also located between the base pairs. Accordingly, 7-hydroxycoumarin was located in the hydrophobic environment and directed towards the phosphate anions of the complementary strand, which enhanced protonation upon hybridization.

2.3. Preparation of a quencher-free molecular beacon by introducing 7-hydroxycoumarin into the stem region

7-Hydroxycoumarin quenched its fluorescence upon hybridization. This quenching system can be utilized for the design of a molecular beacon (Scheme 3). We introduced 7-hydroxycoumarin into the stem region of the MB. In the absence of the target, the stem part should form a duplex, and thus the emission of this MB is quenched in the closed state because the dye is protonated. On the other hand, when the complementary target is added, the MB opens and the dye is in the single-stranded state. Therefore, the dye is deprotonated and the emission from 7-hydroxycoumarin should be observed. Consequently, the emission of 7-hydroxycoumarin should turn on in the presence of the target, that is, the dye positively responds to the target.

In 'conventional' MBs, dyes were introduced into the termini. However, in our design, it is necessary to introduce the dye into the middle of the stem region to create a negatively charged and hydrophobic microenvironment around the dye for efficient quenching by protonation. We synthesized five MBs that have 8-mer stem regions with a shared-stem design[37] (Scheme 1). We used the survivin gene as the target DNA, which is highly expressed in breast cancer (**Surv** in Scheme 1).[38] The melting temperatures of all the MBs with and without the target are listed Table S1 in Supplementary data. **MB1**, **MB2**, and **MB3** have a single dye in the stem region at different positions while **MB4** has two dyes to raise the emission intensity. **MBt** is the control MB which has a tethered the dye at its 5′ terminus. In **MBt**, the dye is located outside the DNA duplex even in the closed state. Accordingly, the emission should be observed even in the absence of the target.

Figure 7A shows the emission spectra of **MB1**, which gave weak emission without the target because the dye was protonated in the closed state (solid line). In contrast, when the target was added, strong emission was observed from the deprotonated coumarin at around 465 nm (dotted line). The ratio of the intensities between the open and closed states (S/B ratio) was 10.0 (Table 2). This value is comparable to the ratio of the intensity of **CXG** to that of **CXG**/**cCXG** (15.3). **MB2** and **MB3**, each of which has the dye at different positions, showed similar S/B ratios to **MB1** (8.3 and 7.3, respectively). Thus, MB with 7-hydroxycoumarin in the stem could detect the target in a positive response as designed without significant sequence dependence (see Fig. S3 in Supplementary data for actual data). **MB4** with two dyes also showed a similar positive response to the target, although its S/B ratio was 6.1. This relatively low S/B ratio was caused by low emission intensity (1.3 times higher than **MB1**) in the open state,[39] probably due the self-quenching of dyes in the single-stranded state.

On the other hand, **MBt**, the control MB, did not show a positive response to the target (Fig. 7B), because strong emission was observed even in the closed state. Since the dye in **MBt** was located

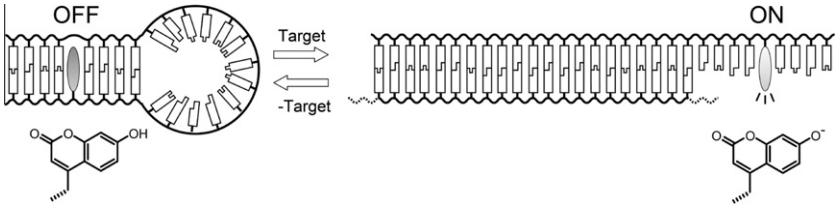

Scheme 3. Schematic illustration of target detection by using an MB with 7-hydroxycoumarin.

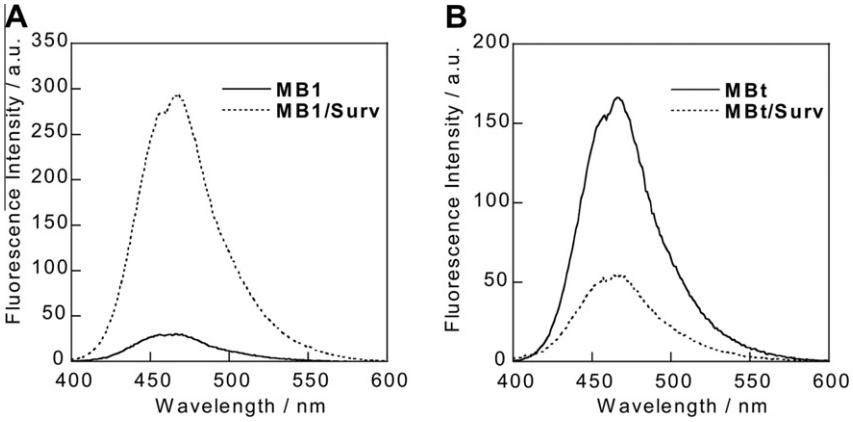

Figure 7. Fluorescence emission spectra (365 nm excitation) of (A) MB1 and (B) MBt with (solid line) and without Surv (dotted line) at pH 8. Solution conditions are as follows: [MB] = 1.0 μM, [Surv] = 2.0 μM, [NaCl] = 100 mM, pH 8.0 (10 mM Tris buffer), 0 °C. The excitation wavelength was 365 nm.

Table 2
Effects of pH on the melting temperature (T_m) of CXG/cCXG and the absorption maxima of single-stranded CXG and CXG/cCXG

Sequence	Relative intensity[a]		*S*/*B* ratio[b]
	Without **Surv**	With **Surv**	
MB1	1	10.0	10.0
MB2	1.1	9.3	8.3
MB3	1.2	8.9	7.3
MB4	2.2	13.3	6.1
MBt	5.6	1.8	0.3

[a] Relative intensity at 465 nm relative to that of **MB1** without **Surv**. Solution conditions: [MB] = 1.0 μM, [**Surv**] = 2.0 μM, [NaCl] = 100 mM, pH 8.0 (10 mM Tris buffer), 0 °C.
[b] Ratio of the fluorescence intensity of the MB in open and closed state.

outside of the duplex, protonation did not occur. The addition of **Surv** did not increase, but actually decreased, the emission of coumarin, probably due to quenching by the neighboring base pairs. Accordingly, incorporation of coumarin into the stem is essential for the design of an MB for positive response.

3. Conclusions

In conclusion, we have successfully developed a simple but efficient quencher-free molecular beacon, only by introducing a single 7-hydroxycoumarin into the middle of the stem region via D-threoninol. UV–Vis and CD spectra of 7-hydroxycoumarin-modified ODN indicated that the dye is intercalated between base pairs. The pK_a of 7-hydroxycoumarin in single-stranded state was 8.8, whereas that in the duplex was more than 10. Consequently, the pK_a change upon hybridization was over 1.2. This large difference could be attributed to electrostatic interactions with phosphate anions in the complementary strand. In addition, the hydrophobic microenvironment between base pairs could also contribute to the pK_a shift.

We incorporated 7-hydroxycoumarin into the stem region of molecular beacons. In the absence of the target, the emission from 7-hydroxycoumarin was quenched due to the protonation. On the other hand, strong emission was observed by the addition of the target. Consequently, the S/B ratio of the molecular beacon was 10.0. In our design of quencher-free MBs based on pK_a change, the incorporation of chromophores into the stem region is essential. Otherwise, quenching of the dye in the closed state does not occur as evidenced by **MBt**.

4. Experimental section

4.1. General

All conventional phosphoramidite monomers, CPG columns, reagents for DNA synthesis, and Poly-Pak II cartridges were purchased from Glen Research. Other reagents for the synthesis of phosphoramidite monomers were purchased from Tokyo Kasei Co., Ltd, and Sigma–Aldrich.

4.1.1. Preparation of compound 2

Compound **1** was synthesized according to a previous report.[4] 7-hydroxycoumarinyl-4-acetic acid (1.33 g, 6.0 mmol) was reacted with PyBOP (3.67 g, 7.1 mmol) and Et_3N (10 ml) in CH_2Cl_2 (30 ml) for 10 min. Then, a solution of compound **1** (2.05 g, 5.0 mmol) in CH_2Cl_2 (10 ml) was added to the above mixture. After vigorous stirring for 3 days, the organic solution was washed with a saturated aqueous solution of $NaHCO_3$. The solvent was removed by evaporation, followed by silica gel column chromatography ($CHCl_3$/MeOH/Et_3N = 60:1:2, R_f = 0.2) to afford **2** (2.90 g, yield 94%). ^{1}H NMR [$CDCl_3$, 500 MHz] δ = 7.49 (d, J = 8.5 Hz, 1H), 7.29–7.18 (m, 9H), 6.82–6.78 (m, 4H), 6.73 (m, 2H), 6.59 (m, 1H), 6.19 (s, 1H), 4.01 (m, 1H), 3.92 (m, 1H), 3.78 (s, 6H), 3.69 (s, 2H), 3.35 (dd, J = 4.5 Hz, 9.5 Hz, 1H), 3.21 (dd, J = 3.5 Hz, 9.5 Hz, 1H), 1.04 (d, J = 6.5 Hz, 3H). ^{13}C NMR [$CDCl_3$, 126 MHz] δ = 169.0, 161.9, 161.1, 158.6, 155.1, 150.0, 144.3, 135.4, 135.3, 129.9, 129.1, 128.0, 127.9, 127.0, 125.8, 113.8, 113.3, 112.6, 111.6, 103.2, 86.7, 67.9, 64.0, 55.2, 54.6, 39.9, 20.1. HRMS(FAB) Calcd for $C_{36}H_{35}NO_8$ (M^+) 609.2363. Found: 609.2343.

4.1.2. Preparation of compound 3

Potassium *tert*-butoxide (0.184 g, 1.64 mmol) was added to a solution of compound **2** (1.0 g, 1.6 mmol) in dry THF (10 ml) under nitrogen. Then, acetic anhydride (0.16 ml, 1.6 mmol) was added to the above mixture. After vigorous stirring overnight, the solvent was removed by evaporation, followed by silica gel column chromatography ($CHCl_3$/MeOH = 60:1, R_f = 0.2) to afford **3** (0.73 g, yield 68%). ^{1}H NMR [$CDCl_3$, 500 MHz] δ = 7.67 (d, J = 8.5 Hz, 1H), 7.34–7.19 (m, 9H), 7.11 (s, 1H), 7.01 (d, J = 8.5 Hz, 1H), 6.81 (m, 4H), 6.44 (m, 1H), 6.38 (s, 1H), 4.05 (m, 1H), 3.94 (m, 1H), 3.77 (s, 6H), 3.68 (s, 2H), 3.35 (dd, J = 4.5 Hz, 9.5 Hz, 1H), 3.27 (dd, J = 4 Hz, 10 Hz, 1H), 2.87 (br, 1H), 2.32 (s, 3H), 1.05 (d, J = 6.5 Hz, 3H). HRMS(FAB) Calcd for $C_{38}H_{37}NO_9$ (M^+) 651.2468. Found: 651.2449.

4.1.3. Preparation of compound 4

Et_3N (0.13 ml, 1.2 mmol) and 2-cyanoethyldiisopropylchloro phosphoramidite (0.075 ml, 0.34 mmol) were added to a solution of compound **3** (0.20 g, 0.31 mmol) in CH_3CN (5.0 ml) at 0 °C under nitrogen. After 20 min of vigorous stirring, the solution was stirred for 1 h at room temperature. Then, an excess of AcOEt was added to the reaction mixture which was washed with a saturated aqueous solution of $NaHCO_3$ and of NaCl. After drying over $MgSO_4$, the solvent was removed by evaporation. The oily product **4** was used for DNA synthesis without further purification. ^{31}P NMR [121 MHz, $CDCl_3$] δ = 148.7, 147.8. HRMS(FAB) Calcd for $C_{47}H_{55}N_3O_{10}P$ ($M+H^+$) 852.3625. Found: 852.3647.

4.2. DNA synthesis

All of the modified DNAs were synthesized on an automated DNA synthesizer (ABI-3400 DNA synthesizer, Applied Biosystems) by using phosphoramidite monomers bearing dye molecules. The coupling efficiency of the monomers corresponding to the modified residues was as high as that of the conventional monomers, as judged from the coloration of the released trityl cation. The acetyl group protecting the hydroxyl group of 7-hydroxycoumarin was deprotected by treatment with an ammonium hydroxide solution at 55 °C for 8 h. After the recommended workup, they were purified by reversed phase (RP)-HPLC and were characterized by MALDI-TOFMS (Autoflex, Bruker Daltonics). The MALDI-TOFMS data for the DNAs were as follows: **CXG**: Obsd 4015 (Calcd for [**CXG**+H^+]: 4014). **MB1**: Obsd 9319 (Calcd for [**MB1**+H^+]: 9318). **MB2**: Obsd 9317 (Calcd for [**MB2**+H^+]: 9318). **MB3**: Obsd 9319 (Calcd for [**MB3**+H^+]: 9318). **MB4**: Obsd 9687 (Calcd for [**MB4**+H^+]: 9687). **MBt**: Obsd 9319 (Calcd for [**MBt**+H^+]: 9318).

4.3. Spectroscopic measurements

UV–Vis and CD spectra were measured on a JASCO model V-530 and J-820, respectively, with a 10-mm quartz cell that was equipped with programmed temperature-controllers. The sample solutions were as follows: [NaCl] = 100 mM, [DNA] = 5.0 or 10.0 μM. Fluorescence spectra were measured on a JASCO model FP-6500 with a microcell. The excitation wavelength was 365 nm. The sample solutions were as follows: [NaCl] = 100 mM, [DNA] = 1.0, 2.0 or 5.0 μM. For measurements at pH 7.0, 8.0–9.5, or 10.0, 10 mM phosphate, Tris, or CAPS (*N*-cyclohexyl-3-aminopropanesulfonic acid) buffer was used, respectively.

4.4. Measurement of the melting temperature

The melting curve of duplex DNA was obtained with a JASCO V-530 by measurement of the change in absorbance at 260 nm versus temperature. The melting temperature (T_m) was determined from the maximum in the first derivative of the melting curve. Both the heating and the cooling curves were measured, and the calculated T_ms agreed to within 2.0 °C. The temperature ramp was 1.0 °C min^{-1}. The sample solutions were as follows: [NaCl] = 100 mM, [DNA] = 5.0 μM. For measurements at pH 7.0, 8.0–9.5, or 10.0, 10 mM phosphate, Tris, or CAPS (*N*-cyclohexyl-3-aminopropanesulfonic acid) buffer was used, respectively. Quantum yield was determined from the quantum yield of 7-hydroxy-4-methylcoumarin in 0.1 M phosphate buffer at pH 10 (0.63) as a reference.[26]

4.5. Titration experiments

The pK_a was determined from the absorbance of the sample at 20 °C. The pH was adjusted by adding small amounts of conc. NaOH solution to the sample. Conditions of the sample solutions were as follows: [NaCl] = 100 mM, [Na_2HPO_4/NaH_2PO_4] = 10 mM. Since pH titration could not be conducted at a pH higher than 10 due to the dissociation of the duplex, pK_a was determined by assuming the following equation with a curve-fitting program using KaleidaGraph 3.5 (Synergy Software):

$$A = A_{HA} + \frac{(A_{A^-} - A_{HA})}{10^{(pK_a - pH)}}$$

where A_{HA} and A_{A^-} denote the absorbances of fully protonated and deprotonated forms.

Acknowledgments

This work was partially supported by a Grant-in-Aid for Scientific Research (A) (21241031) and a Grant-in-Aid for Young Scientists (B) (22750149) from the Ministry of Education, Culture, Sports, Science and Technology, Japan. Partial supports by SENTAN program (JST) and The Asahi Glass Foundation are also acknowledged.

Supplementary data

Supplementary data associated with this article can be found, in the online version, at http://dx.doi.org/10.1016/j.bmc.2012.05.052.

References and notes

1. Tyagi, S.; Kramer, F. R. *Nat. Biotechnol.* **1996**, *14*, 303.
2. Wang, K.; Tang, Z.; Yang, C. J.; Kim, Y.; Fang, X.; Li, W.; Wu, Y.; Medley, C. D.; Cao, Z.; Li, J.; Colon, P.; Lin, H.; Tan, W. *Angew. Chem., Int. Ed.* **2009**, *48*, 856.
3. Kashida, H.; Takatsu, T.; Fujii, T.; Sekiguchi, K.; Liang, X.; Niwa, K.; Takase, T.; Yoshida, Y.; Asanuma, H. *Angew. Chem., Int. Ed.* **2009**, *48*, 7044.
4. Hara, Y.; Fujii, T.; Kashida, H.; Sekiguchi, K.; Liang, X.; Niwa, K.; Takase, T.; Yoshida, Y.; Asanuma, H. *Angew. Chem., Int. Ed.* **2010**, *49*, 5502.
5. Venkatesan, N.; Seo, Y. J.; Kim, B. H. *Chem. Soc. Rev.* **2008**, *37*, 648.
6. Hwang, G. T.; Seo, Y. J.; Kim, B. H. *J. Am. Chem. Soc.* **2004**, *126*, 6528.
7. Ryu, J. H.; Seo, Y. J.; Hwang, G. T.; Lee, J. Y.; Kim, B. H. *Tetrahedron* **2007**, *63*, 3538.
8. Saito, Y.; Mizuno, E.; Bag, S. S.; Suzuka, I.; Saito, I. *Chem. Commun.* **2007**, 4492.
9. Matsumoto, K.; Shinohara, Y.; Bag, S. S.; Takeuchi, Y.; Morii, T.; Saito, Y.; Saito, I. *Bioorg. Med. Chem. Lett.* **2009**, *19*, 6392.
10. Heinlein, T.; Knemeyer, J.-P.; Piestert, O.; Sauer, M. *J. Phys. Chem. B* **2003**, *107*, 7957.
11. Østergaard, M. E.; Cheguru, P.; Papasani, M. R.; Hill, R. A.; Hrdlicka, P. J. *J. Am. Chem. Soc.* **2010**, *132*, 14221.
12. Nazarenko, I.; Lowe, B.; Darfler, M.; Ikonomi, P.; Schuster, D.; Rashtchian, A. *Nucleic Acids Res.* **2002**, *30*, e37.
13. Tyagi, S.; Marras, S. A. E.; Kramer, F. R. *Nat. Biotechnol.* **2000**, *18*, 1191.
14. Li, X.; Li, Z.; Marti, A. A.; Jockusch, S.; Stevens, N.; Akins, D. L.; Turro, N. J.; Ju, J. *Photochem. Photobiol. Sci.* **2006**, *5*, 896.
15. Martí, A. A.; Jockusch, S.; Li, Z.; Ju, J.; Turro, N. J. *Nucleic Acids Res.* **2006**, *34*, e50.
16. Zhang, P.; Beck, T.; Tan, W. *Angew. Chem., Int. Ed.* **2001**, *40*, 402.
17. Varghese, R.; Wagenknecht, H.-A. *Org. Biomol. Chem.* **2010**, *8*, 526.
18. Socher, E.; Bethge, L.; Knoll, A.; Jungnick, N.; Herrmann, A.; Seitz, O. *Angew. Chem., Int. Ed.* **2008**, *47*, 9555.
19. Fujimoto, K.; Shimizu, H.; Inouye, M. *J. Org. Chem.* **2004**, *69*, 3271.
20. Seo, Y. J.; Hwang, G. T.; Kim, B. H. *Tetrahedron Lett.* **2006**, *47*, 4037.
21. Berndl, S.; Wagenknecht, H.-A. *Angew. Chem., Int. Ed.* **2009**, *48*, 2418.
22. Knemeyer, J.-P.; Marmé, N.; Häfner, B.; Habl, G.; Schäfer, G.; Müller, M.; Nolte, O.; Sauer, M.; Wolfrum, J. *Int. J. Environ. Anal. Chem.* **2005**, *85*, 625.
23. Asanuma, H.; Kashida, H.; Liang, X. G.; Komiyama, M. *Chem. Commun.* **2003**, 1536.
24. Kashida, H.; Sano, K.; Hara, Y.; Asanuma, H. *Bioconjugate Chem.* **2009**, *20*, 258.
25. Adamczyk, M.; Cornwell, M.; Huff, J.; Rege, S.; Rao, T. V. S. *Bioorg. Med. Chem. Lett.* **1985**, *1997*, 7.
26. Sun, W.-C.; Gee, K. R.; Haugland, R. P. *Bioorg. Med. Chem. Lett.* **1998**, *8*, 3107.
27. Seela, F.; Sirivolu, V. R.; Chittepu, P. *Bioconjugate Chem.* **2008**, *19*, 211.
28. Seela, F.; Sirivolu, V. R. *Org. Biomol. Chem.* **2008**, *6*, 1674.
29. Sirivolu, V. R.; Chittepu, P.; Seela, F. *ChemBioChem* **2008**, *9*, 2305.
30. Seela, F.; Xiong, H.; Leonard, P.; Budow, S. *Org. Biomol. Chem.* **2009**, *7*, 1374.
31. Kashida, H.; Liang, X. G.; Asanuma, H. *Curr. Org. Chem.* **2009**, *1065*, 13.
32. Nishioka, H.; Liang, X.; Asanuma, H. *Chem. Eur. J.* **2010**, *16*, 2054.
33. Liang, X. G.; Asanuma, H.; Kashida, H.; Takasu, A.; Sakamoto, T.; Kawai, G.; Komiyama, M. *J. Am. Chem. Soc.* **2003**, *125*, 16408.
34. Fujii, T.; Kashida, H.; Asanuma, H. *Chem. Eur. J.* **2009**, *15*, 10092.
35. Lying, R.; Rodger, A.; Nordén, B. *Biopolymers* **1991**, *31*, 1709.
36. Lyng, R.; Rodger, A.; Nordén, B. *Biopolymers* **1992**, *32*, 1201.
37. Tsourkas, A.; Behlke, M. A.; Bao, G. *Nucleic Acids Res.* **2002**, *30*, 4208.
38. Peng, X.-H.; Cao, Z.-H.; Xia, J.-T.; Carlson, G. W.; Lewis, M. M.; Wood, W. C.; Yang, L. *Cancer Res.* **1909**, *2005*, 65.
39. Emission intensity of **MB4** with two dyes in the closed state was almost doubled.